0026-895X/10/7704-508–516
MOLECULAR PHARMACOLOGY
U.S. Government work not protected by U.S. copyright
Mol Pharmacol 77:508–516, 2010

Vol. 77, No. 4
62356/3568760
Printed in U.S.A.

Human Carboxylesterase 1 Stereoselectively Binds the Nerve Agent Cyclosarin and Spontaneously Hydrolyzes the Nerve Agent Sarin

Andrew C. Hemmert, Tamara C. Otto, Monika Wierdl, Carol C. Edwards, Christopher D. Fleming, Mary MacDonald, John R. Cashman, Philip M. Potter, Douglas M. Cerasoli, and Matthew R. Redinbo

Departments of Chemistry (M.R.R.) and Biochemistry and Biophysics (A.C.H., C.D.F., M.R.R.), University of North Carolina at Chapel Hill, Chapel Hill, North Carolina; U.S. Army Medical Research Institute of Chemical Defense (T.C.O., D.M.C.), Aberdeen Proving Ground, Maryland; Human BioMolecular Research Institute (M.M., J.R.C.), San Diego, California; and Department of Molecular Pharmacology (M.W., C.C.E., P.M.P.), St. Jude Children's Research Hospital, Memphis, Tennessee

Received November 12, 2009; accepted January 5, 2010

ABSTRACT

Organophosphorus (OP) nerve agents are potent toxins that inhibit cholinesterases and produce a rapid and lethal cholinergic crisis. Development of protein-based therapeutics is being pursued with the goal of preventing nerve agent toxicity and protecting against the long-term side effects of these agents. The drug-metabolizing enzyme human carboxylesterase 1 (hCE1) is a candidate protein-based therapeutic because of its similarity in structure and function to the cholinesterase targets of nerve agent poisoning. However, the ability of wild-type hCE1 to process the G-type nerve agents sarin and cyclosarin has not been determined. We report the crystal structure of hCE1 in complex with the nerve agent cyclosarin. We further use stereoselective nerve agent analogs to establish that hCE1 exhibits a 1700- and 2900-fold preference for the P_R enantiomers of analogs of soman and cyclosarin, respectively, and a 5-fold preference for the P_S isomer of a sarin analog. Finally, we show that for enzyme inhibited by racemic mixtures of bona fide nerve agents, hCE1 spontaneously reactivates in the presence of sarin but not soman or cyclosarin. The addition of the neutral oxime 2,3-butanedione monoxime increases the rate of reactivation of hCE1 from sarin inhibition by more than 60-fold but has no effect on reactivation with the other agents examined. Taken together, these data demonstrate that hCE1 is only reactivated after inhibition with the more toxic P_S isomer of sarin. These results provide important insights toward the long-term goal of designing novel forms of hCE1 to act as protein-based therapeutics for nerve agent detoxification.

Originally discovered in 1854 as potent pesticides, organophosphorus (OP) nerve agents are some of the deadliest chemical compounds ever synthesized by humans (Newmark, 2007). During the Iran-Iraq war, Iranian soldiers were targeted with several chemical weapons, including sulfur mustard and the OP nerve agent sarin (*O*-isopropyl methylphosphonofluoridate). In 1988, Saddam Hussein used sarin and the related OP agent tabun (ethyl *N,N*-dimethylphosphoramidocyanidate) against Kurdish citizens in Halabja, killing 5000 (Newmark, 2007). More recently, the cult Aum Shinrikyo released diluted sarin in the Tokyo subway system in 1995, killing 12 and affecting thousands (Okumura et al., 2005). Even though these and related compounds were banned by the 1997 Chemical Weapons Warfare Convention, their ease of synthesis and known use by rogue nations and terrorist groups continue to pose a security threat (Trapp, 2006).

OP nerve agents are alkylphosphonic esters (Fig. 1) that covalently modify a variety of enzymes, most importantly the neurotransmitter regulating enzyme acetylcholinesterase

This work was supported by the National Institutes of Health National Institute of Neurological Disorders and Stroke [Grant NS58089]; the National Institutes of Health National Cancer Institute [Grant CA21765]; and the American Lebanese Syrian Associated Charities.

Portions of these data were presented previously in poster and presentation formats at the CounterACT Network Research Symposium in Washington, DC, 14-16 Apr 2009.

Article, publication date, and citation information can be found at http://molpharm.aspetjournals.org.

doi:10.1124/mol.109.062356.

ABBREVIATIONS: OP, organophosphorus; sarin, *O*-isopropyl methylphosphonofluoridate; tabun, ethyl *N,N*-dimethylphosphoramidocyanidate; AChE, human acetylcholinesterase; soman, *O*-pinacolyl methylphosphonofluoridate; cyclosarin, *O*-cyclohexyl methylphosphonofluoridate; BuChE, human butyrylcholinesterase; hCE1, human carboxylesterase 1; DAM, 2,3-butanedione monoxime; RMSD, root mean square deviation; pNPB, *para*-nitrophenyl butyrate; RCSB PDB, Research Collaboratory for Structural Bioinformatics Protein Data Bank.

(AChE). AChE inhibition leads to continual acetylcholine stimulus of the muscarinic and nicotinic receptors, resulting in seizures, convulsions, diaphragm incapacitation, and, in cases of higher-dose exposure, death. After phosphonylation of the catalytic serine in AChE, a spontaneous, time-dependent dealkylation may occur (known as aging), resulting in a stable phosphonylated enzyme that is resistant to recovery therapies (Jokanovic, 2009). The P_S enantiomers of sarin, soman (*O*-pinacolyl methylphosphonofluoridate), and cyclosarin (*O*-cyclohexyl methylphosphonofluoridate) are significantly more lethal than the P_R isomers because of their preferential inhibition of the AChE enzyme (Kovarik et al., 2003).

Current treatments for nerve agent poisoning include injections of atropine, a competitive inhibitor of acetylcholine at the muscarinic receptor, to turn off muscle stimulus, and a strong nucleophilic oxime such as pralidoxime chloride, to dephosphonylate the AChE catalytic serine before aging (Gray, 1984). Both of the compounds offer limited protection because they cannot be administered before exposure and do not address any of the long-term side effects associated with nerve agent poisoning (Doctor and Saxena, 2005). Prophylactic protein-based therapeutics are emerging as a means to protect against both toxicity and long-term side effects in nerve agent poisoning (Lenz et al., 2007). These biological reagents act as "bioscavengers" to stoichiometrically sequester nerve agents before AChE inhibition (Dunn and Sidell, 1989). Preadministration of excess bioscavenger in mice provides protection against mortality equivalent to a postexposure oxime injection but is superior at minimizing postexposure effects such as lacrimation or decreased motor function (Maxwell et al., 1993; Doctor and Saxena, 2005). Current stoichiometric bioscavengers include AChE and the related serine hydrolase butyrylcholinesterase (BuChE). A more advanced protein-based therapeutic would include a catalytic function to detoxify nerve agents before AChE inhibition reaches lethal levels. For example, human serum paraoxonase and bacterial organophosphorus hydrolase are being studied for this application (Lenz et al., 2007; Reeves et al., 2008).

Human carboxylesterase 1 (hCE1) is a 62-kDa serine hydrolase belonging to the same α/β hydrolase superfamily as AChE and BuChE but may offer some benefits over cholinesterases as a potential catalytic nerve agent, hydrolase. Indeed, high-serum carboxylesterase concentrations in rodents and mosquitoes protect these species from OP nerve agent exposure (Maxwell, 1992; Heidari et al., 2004). hCE1, found primarily in the liver, uses a catalytic triad composed of a serine, histidine, and glutamic acid in a standard two-step serine hydrolase catalytic mechanism. hCE1 cleaves ester, thioester, and amine-ester bonds in a variety of endogenous and xenobiotic compounds (Redinbo and Potter, 2005). We published previously the crystal structures of hCE1 in covalent acyl-enzyme complexes with the nerve agents soman and tabun (Fleming et al., 2007). However, the ability of hCE1 to reverse covalent inhibition and reactivate wild-type activity was not examined in that study.

Here we present a 3.1-Å X-ray nonaged crystal structure of hCE1 in covalent complex with the nerve agent cyclosarin, the first structure determined of any protein bound to this agent. To further examine the potential of hCE1 as either a bioscavenger or a nerve agent hydrolase, we used bona fide nerve agents and stereogenic analogs thereof to measure the bimolecular rates of inhibition and the spontaneous and oxime-assisted rates of reactivation of hCE1 in the presence of sarin, soman, and cyclosarin. Last, we examine the propensity of hCE1 to age in the presence of nerve agent adducts. These crystallographic and biochemical data advance our understanding of the ability of hCE1 to process organophosphorus compounds and will assist in the potential devel-

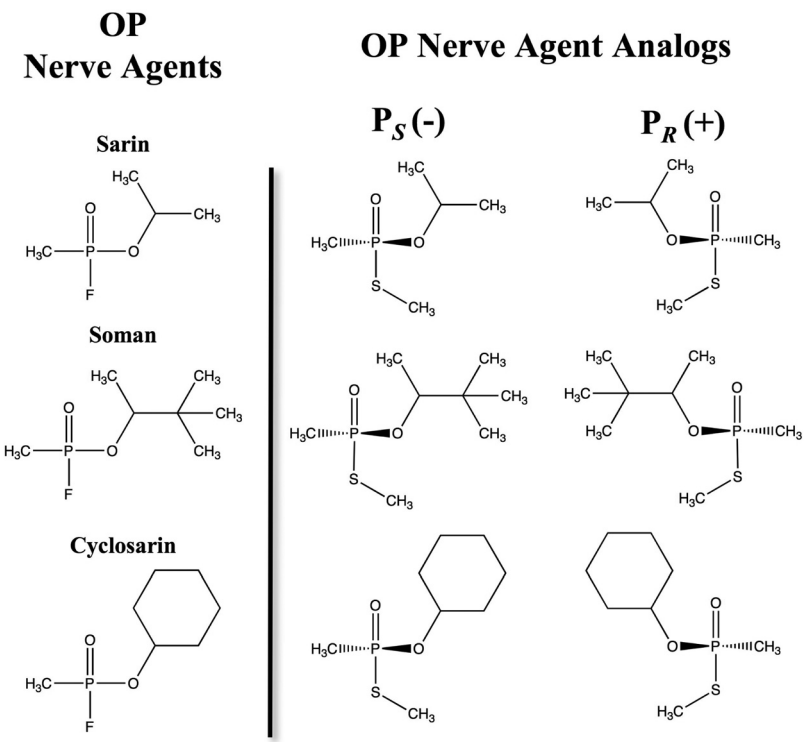

Fig. 1. Organophosphate nerve agents and nerve agent analogs. Nerve agents contain a methyl, *O*-alkoxy, and good leaving group built on a central chiral phosphonate. The stereogenic OP nerve agent analogs contain a thiomethyl leaving group in place of the fluoride.

opment of this enzyme as a protein-based therapeutic to prevent nerve agent toxicity.

Materials and Methods

Nerve Agent Inhibition and Crystallization. hCE1 was expressed and secreted from baculovirus-infected *Spodoptera frugiperda* Sf21 cells and purified to >98% homogeneity by SDS-polyacrylamide gel electrophoresis as described previously (Morton and Potter, 2000). At the United States Army Medical Research Institute of Chemical Defense (Aberdeen Proving Ground, MD), 2 mg of purified protein was incubated with ~10-fold molar excess of racemic cyclosarin (obtained from the Research Development and Engineering Command, Aberdeen Proving Ground, MD) for 1 h at room temperature. Excess unbound agent was removed by passing inhibited hCE1 over a PD-10 Sephadex G-25 size exclusion chromatography column (GE Healthcare, Chalfont St. Giles, Buckinghamshire, UK). Postcolumn samples were tested to confirm complete inhibition by measuring hydrolysis of *para*-nitrophenyl butyrate (pNPB; Sigma-Aldrich, St. Louis, MO), a conventional esterase substrate (Wierdl et al., 2008). To assess the extent to which excess cyclosarin was retained within the column, the capacity of the eluate to subsequently inhibit BuChE was also determined. Cyclosarin-inhibited hCE1 was concentrated to 3 mg/ml using Amicon Ultra-15 (Millipore, Billerica, MA) spin concentrators. Plate-like crystals (600 × 100 × 50 μM) were grown in 4 to 6 weeks using the sitting drop vapor-diffusion method in 10% polyethylene glycol 3350, 0.3 M Li_2SO_4, 0.1 M citrate, pH 5.5, 0.1 M NaCl, 0.1 M LiCl, and 5% glycerol. Before cooling to 100 K in liquid nitrogen, crystals were cryoprotected by stepwise passages into a final concentration of 30% (w/v) sucrose plus mother liquor.

Structure Determination and Refinement. X-Ray diffraction data were collected at 100 K at the Advanced Photon Source at Argonne National Laboratory (Argonne, IL) on beam line 22-ID (Southeast Regional Collaborative Access Team, Argonne National Laboratory). Data were indexed and scaled using the XDS package (Kabsch, 1988). Molecular replacement was conducted using MolRep in the CCP4i suite (Collaborative Computational Project, 1994) (version 6.1.0) with one trimer of the hCE1-tacrine structure (RCSB PDB access code 1mx1; Bencharit et al., 2003) as the search model. The hCE1-cyclosarin model was refined using rigid body, simulated annealing, and grouped *B*-factor refinements in the Crystallography and NMR System (Brünger et al., 1998) that included an overall anisotropic *B*-factor, bulk solvent correction, and noncrystallographic symmetry restraints for regions outside the active site. Before any structural refinement, a subset (7%) of the data was set aside for cross-validation by R_{free} calculation. Manual building was conducted in Coot (Emsley and Cowtan, 2004) with σ_a-weighted composite omit, difference density, and simulated annealing omit maps. Data collection and refinement statistics were summarized and are presented in Table 1. The final structure was validated using PROCHECK (Laskowski et al., 1993), and all figures were generated in PyMol (DeLano Scientific, Palo Alto, CA). Coordinates and structure factors were deposited at the PDB with access code 3k9b.

Inhibition Rate Constants Using Nerve Agent Analogs. Samples of purified hCE1 at 100 nM were inhibited at room temperature with increasing concentrations of stereogenic OP nerve agent analogs. Aliquots of enzyme incubated with stereoisomer analogs of sarin (P_R, P_S), P_S soman, and P_S cyclosarin were removed at various time points (up to 1 h), and the level of active enzyme that remained was determined by comparing pNPB hydrolysis relative to an uninhibited sample. Because the P_R soman and P_R cyclosarin analogs react more quickly with hCE1, the affects these analogs had on hCE1 were measured continuously (for up to 15 min) by adding increasing concentrations of analog to hCE1 samples containing pNPB and by measuring the loss of functional enzyme activity over time. These data, collected at 410 nm and 25°C on a Pherastar microplate reader (BMG Labtech, Durham, NC), were corrected for spontaneous pNPB hydrolysis and fit to eq. 1 (Aurbek et al., 2006):

$$\frac{\Delta t}{\Delta \ln \nu} = \frac{K_d}{k_2} \cdot \frac{1}{[IX](1-\alpha)} + \frac{1}{k_2} \quad (1)$$

where K_d is the dissociation constant, k_2 is the unimolecular phosphorylation rate constant, υ is the remaining percentage of enzyme activity, [IX] is the OP analog concentration, α is [S]/(K_M + [S]), in which [S] is the substrate concentration and K_M is the Michaelis-Menten constant. All experiments were performed in triplicate. Data were analyzed using KaleidaGraph 4 (Synergy Software, Reading, PA) to determine k_i ($k_i = k_2/K_d$) values.

Spontaneous Reactivation. Fifty microliters of COS cell lysate expressing a nonsecreted form of hCE1, prepared as described previously (Wierdl et al., 2008), was inhibited with a ~1000-fold molar excess of racemic OP agents sarin, soman, or cyclosarin for 10 min. Excess agent was removed by passing inhibited samples over a PD-10 Sephadex G-25 exclusion column (GE Healthcare). The column eluate was diluted 10-fold in 0.1 M potassium phosphate buffer, pH 7.4, and tested for the presence or absence of carboxylesterase activity and complete removal of excess agent, as described previously. Aliquots were removed over time (up to 80 h), and the percentage of enzyme activity was measured by pNPB hydrolysis relative to an uninhibited sample. The rate of reactivation (k_{obs}) and maximal percentage of recovery (A_{max}) were determined by fitting the data to eq. 2:

$$A = A_0 + A_{max}(1 - e^{-k_{obs}t}) \quad (2)$$

where A is the percentage of activity at time t, and A_0 is the initial activity at $t = 0$. The experiments were conducted in triplicate, and data were analyzed using Sigma Plot version 8.02 (Systat Software Inc., San Jose, CA).

Oxime-Assisted Reactivation. Fifty microliters of COS cell lysate containing hCE1 was inhibited, and excess agent was removed as described previously. Stereogenic OP analogs were used in a fashion similar to that of racemic nerve agents but required a longer incubation time (up to 1 h). Upon column elution, samples were diluted 10-fold into 1 mM 2,3-butanedione monoxime (DAM; Sigma-Aldrich), which had been prepared previously in 0.1 M potassium

TABLE 1
Crystallographic data collection and refinement statistics

	Statistic
X-ray data collection	
Space group	$P2_12_12_1$
Cell dimensions	
a, b, c (Å)	55.6, 179.9, 200.6
α, β, γ (°)	90.0, 90.0, 90.0
Resolution (Å) (highest shell)	48–3.1 (3.3–3.1)[a]
R_{sym} (%)[b]	13.1 (48.1)
I/σ	13.6 (4.5)
Completeness (%)	97.5 (94.0)
Redundancy	7.0 (6.2)
Crystallographic refinement	
Resolution (Å)	48–3.1 (3.3–3.1)
Unique reflections	36,488
Mean thermal displacement parameter (Å^2)	
Protein	53.9
Water	49.2
Root-mean-square deviation	
Bond lengths (Å)	0.014
Bond angles (°)	1.70
R_{work}/R_{free} (%)[c,d]	26.6 (26.8)/29.9 (29.6)

[a] Number in parentheses is for the highest shell.
[b] $R_{sym} = \Sigma|I - \langle I\rangle|\Sigma\ I$, where I is the observed intensity and $\langle I\rangle$ is the average intensity of multiple symmetry-related observations of that reflection.
[c] $R_{work} = \Sigma\ ||F_o| - |F_c||/\Sigma|F_o|$, where F_o and F_c are the observed and calculated structure factors, respectively.
[d] $R_{free} = \Sigma\ ||F_o| - |F_c||/\Sigma|F_o|$ for 7% of the data not used at any stage of structural refinement.

phosphate, pH 7.4, and kept on ice. DAM had no inhibitory effect on hCE1 at this concentration (data not shown). Aliquots were removed over time, and enzyme activity was measured as described above. The rate of reactivation (k_{obs}) and maximal percentage of reactivation (A_{max}) were determined for each agent/analog by subtracting background oxime-induced pNPB hydrolysis and fitting the data to eq. 2.

Aging. Samples of 1 μM purified hCE1 were inhibited with a 1000-fold molar excess of the P_S sarin, soman, and cyclosarin analogs for 60 min at room temperature. Complete inhibition was verified by the absence of pNPB hydrolysis. Excess unbound agent was removed by size-exclusion chromatography as described previously, and aliquots were diluted 1:10 into 1 mM DAM every 12 h for 48 h. After dilution into DAM, each sample was incubated for 24 h to achieve maximal DAM-assisted reactivation, and then enzyme activity was measured and the percentage of reactivation was determined relative to an uninhibited sample. Maximum percentage of reactivation (A_{max}) was plotted against the incubation time in the absence of DAM and fitted to eq. 3 (Shafferman et al., 1996):

$$A_{max} = A_{max0}\exp^{-k_a t} \quad (3)$$

where A_{max0} was the maximum recovery at time = 0, and k_a was the rate of aging.

Results

Crystal Structure of the hCE1-Cyclosarin Complex. The crystal structure of hCE1 in a covalent acyl-enzyme intermediate complex with the OP nerve agent cyclosarin was determined by molecular replacement and refined to 3.1 Å resolution (Table 1). The hCE1-cyclosarin structure was similar to ligand complexes of this enzyme described previously, with a root mean square deviation (RMSD) of 0.48 Å over 1354 equivalent Cα positions compared with the hCE1-tacrine structure (Bencharit et al., 2003). The initial maps were of good quality for the majority of the polypeptide, with the exception of the acyl loop (residues 304–318) that caps the active site and five short loops (340–342, 369–374, 406–410, 450–454, 483–488) between secondary structural elements. When positioned provisionally, these disordered regions displayed *B*-factors of >90 Å^2; in contrast, the average *B*-factor of the ordered regions of the final model was 54 Å^2. Two of these regions (369–374, 450–454) were also disordered in the structure of a rabbit liver carboxylesterase, which shares 81% sequence identity and 0.42 Å RMSD over 401 equivalent Cα positions relative to hCE1 (Bencharit et al., 2002). The model of hCE1 complexed with cyclosarin was refined to final *R* factors of 26.6% (R_{cryst}) and 29.9% (R_{free}) (Table 1).

Each hCE1 monomer, supported by two disulfide links (Cys87–Cys116, Cys274–Cys285), contained two ligand binding sites within three domains: catalytic, α/β, and regulatory (Bencharit et al., 2002) (Fig. 2). The hCE1-trimer was formed through C3 symmetry around respective α/β domains and buries 475 Å^2 of solvent-accessible surface area per protein monomer. The primary ligand binding site, the active site, was located at the interface of the three domains in each monomer and was composed of the Ser221, His468, and Glu354 catalytic triad. The second ligand binding site (or *Z*-site) was on the enzyme's surface at the interface between the regulatory and catalytic domains. Previous crystal structures of hCE1 in complex with OP nerve agents soman and tabun contained sucrose, the cryoprotectant, in the *Z*-site (Fleming et al., 2007). Ser369, which forms a hydrogen bond with the O1 of sucrose in these other structures, was disordered in the hCE1-cyclosarin structure, and no ligand molecule was observed in this site. The catalytic domain also contained a high-mannose glycosylation site at Asn79. Density was observed around Asn79, but neither *N*-acetylglucosamine nor terminal sialic acid could be reliably built and refined into this region.

OP nerve agents inhibit hCE1 by forming a covalent adduct with the catalytic serine (Fig. 3A). In the structure of the hCE1-cyclosarin complex reported here, a covalent cyclosarin adduct was easily identified in initial difference density ($F_o - Fc$) maps as a 6 σ electron density peak approximately 1.6 Å away from the Ser 221 Oγ, which corresponded to the nerve agent phosphate. At lower σ levels (2.5–4 σ), additional density for the complete molecule was apparent. The cyclosarin model was built into the observed density, refined, and P_R stereochemistry was assigned around the chiral phosphate (Fig. 3B). The acyl-enzyme adduct was stabilized by two hydrogen bonds. These occur between the cyclosarin phosphoryl oxygen atom and hydrogen atoms present on the amide nitrogens within residues Gly142 and Gly143 (2.6 and 2.4 Å, respectively). The *O*-cyclohexyl alkoxy group is located within the larger, flexible pocket of the active site and is stabilized by interactions with Leu363 of the regulatory domain. The stereochemistry and alkoxy placement was confirmed with a 3.1-Å resolution simulated annealing omit map, contoured to 5 σ (Fig. 4A). The opposite P_S isomer was also built into the starting model, and one round of refinement was performed. Clear positive and negative density from a difference density map ($|F_o - F_c|$, ϕ_{Calc}) verified the P_R assignment as consistent with the biochemical results (Fig. 4B).

Nerve Agent Analog Stereopreference of hCE1. Sarin, soman, and cyclosarin contain a chiral phosphorus atom and exist as racemic mixtures of P_R and P_S stereoisomers. Soman also has an asymmetric carbon (Cα) in the pinacolyl group. The P_S isomers of sarin, soman, and cyclosarin inhibit AChE more potently than the P_R forms; for example, the preference of P_S versus P_R soman is 5000-fold for AChE (Sanson et al., 2009). Using OP nerve agent analogs containing a thiomethyl-leaving group prepared as purified stereo-

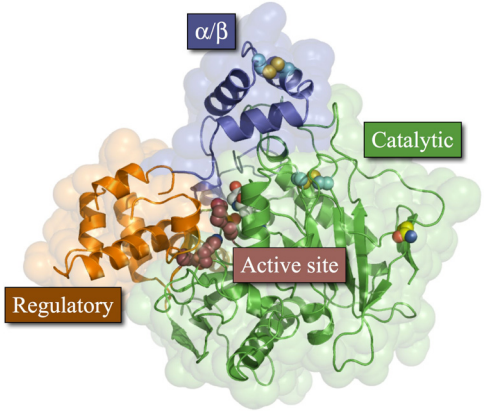

Fig. 2. hCE1 monomer. Each protein monomer has three domains; the α/β domain (blue) forms the trimer interface and caps the active site; the regulatory region (orange) contains the secondary surface binding site (*Z*-site) and Glu354 of the catalytic triad; and the catalytic domain (green) contains the central β-sheet conserved in serine hydrolases and the two catalytic residues His468 and Ser221. There are two disulfide bonds (cyan), one in the α/β domain and the other in the catalytic domain, and one glycosylation site, at Asn79 (yellow).

isomers (Fig. 1), we determined the stereoselectivity of hCE1 inhibition by analogs of sarin, soman, and cyclosarin (Fig. 5). These analogs have been shown by matrix-assisted laser desorption ionization/time of flight mass spectrometry to yield, among other products, acyl-enzyme adducts identical with those from authentic agents when used to inhibit butyrylcholinesterase (Gilley et al., 2009). The thiomethyl-leaving group that replaces the fluoride atom found in nerve agents decreases the toxicity of the analogs by slowing the rate of phosphonylation (k_2) compared with real agents; however, the dissociation constants (K_d) remain similar (Forsberg and Puu, 1984). The decrease in k_2 results in a reduction in the bimolecular rate of inhibition (k_i) by 2 to 3 orders of magnitude compared with the corresponding nerve agent (Maxwell, 1992). P_R analogs of soman and cyclosarin inhibited hCE1 1700- and 2900-fold more efficiently than the P_S isomers, respectively (Fig. 5). In contrast, hCE1 exhibited a 5-fold preference for the P_S versus P_R form of the sarin analogs (Fig. 5). As discussed below, this may be because the smaller *O*-isopropyl group in the sarin analogs is more easily accommodated in the hCE1 active site than that larger *O*-pinacolyl and *O*-cyclohexyl groups of the soman and cyclosarin analogs, respectively. Taken together, these results demonstrate that hCE1 exhibits a strong preference for the P_R soman and cyclosarin analogs and a smaller preference for the P_S isomer of the smaller sarin analog.

Spontaneous Reactivation of hCE1. After the formation of the acyl-enzyme intermediate, proteins exposed to OP nerve agents may remain stably adducted, permanently inhibited (aged), or undergo spontaneous hydrolysis (hereafter referred to as reactivation) reversing the phosphonylation and returning the enzyme to normal function (Langenberg et al., 1988; Li et al., 2007). To test the ability of hCE1 to reactivate after inhibition by nerve agents, the enzyme was challenged with racemic mixtures of the OP nerve agents soman, sarin, and cyclosarin. We found that only samples inhibited with sarin exhibited spontaneous reactivation (Fig. 6A), with a half-time of 45 h ($k_{obs} = 2.58 \pm 0.06 \times 10^{-4}$/min). When carried out to 300 h, a maximum activity of 84 ± 6% was recovered (data not shown). The rate of reactivation was approximately 10-fold slower than that measured for rat serum carboxylesterase (Maxwell and Brecht, 2001) but 10-fold faster than BuChE (Bartling et al., 2007). In contrast, AChE exhibits no reactivation after sarin inhibition (Bartling et al., 2007). hCE1 inhibited with soman and cyclosarin, however, exhibited poor reactivation and achieved a maximum recovery of activity of only ~10% even after 300 h (Fig. 6A). These data establish that reactivation of hCE1 only occurs after exposure to sarin.

Oxime-Assisted Reactivation of hCE1. Strong oxime nucleophiles like pralidoxime chloride and obidoxime are known to reactivate OP-inhibited esterases, particularly AChE, by promoting the dephosphonylation of the active site serine. These cationic oximes are currently used as part of postexposure therapy and are appropriate for the anionic choline binding gorge in cholinesterases (Volans, 1996). Carboxylesterases such as hCE1 react poorly with charged substrates (Maxwell et al., 1994); however, the ability of a neutral oxime like DAM to reactivate inhibited hCE1 has not been reported in the literature. Thus, we tested whether DAM would reactivate hCE1 that had been exposed to racemic mixtures of OP nerve agents. We found that DAM enhanced the reactivation of sarin-inhib-

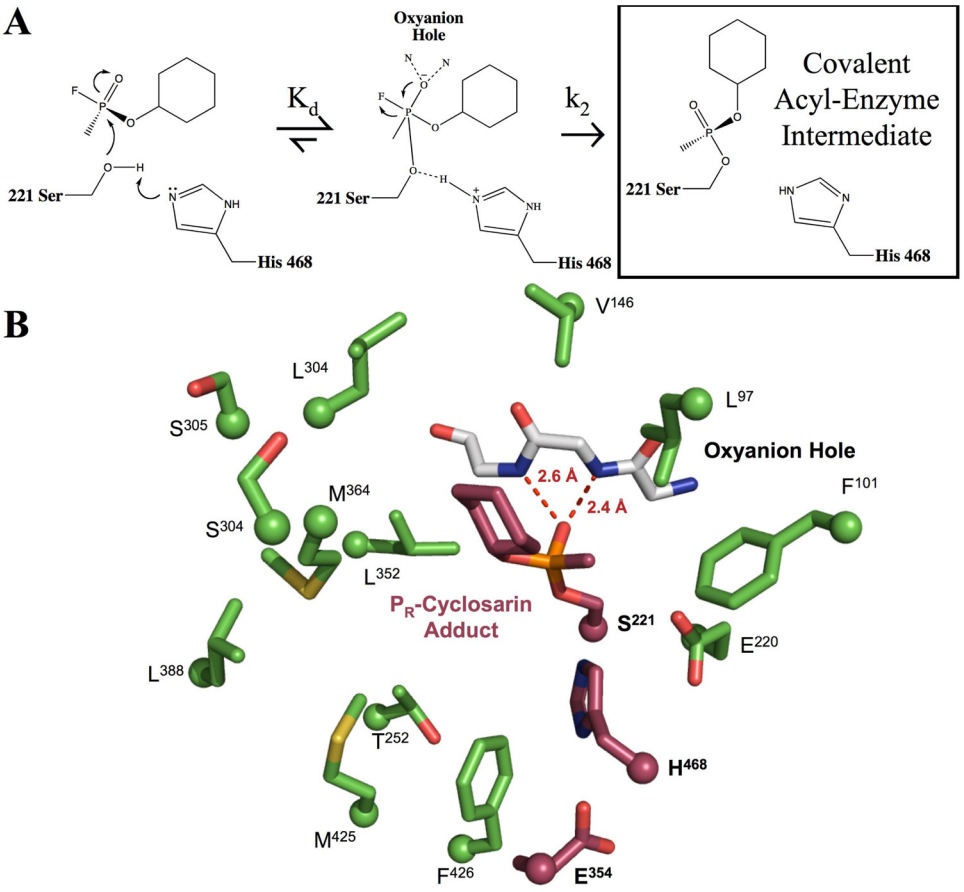

Fig. 3. hCE1-cyclosarin complex. A, chemical scheme of hCE1 reacting with cyclosarin. B, cut-away view of the hCE1-cyclosarin active site. The catalytic triad and cyclosarin molecule are shown in purple, oxyanion hole in white, and the surrounding residues in green. Hydrogen bonds between the phosphoryl oxygen and the backbone nitrogen atoms in the oxyanion hole are shown in red.

ited hCE1 but not enzyme inhibited by soman or cyclosarin (Fig. 6B). In the presence of DAM, sarin-inhibited hCE1 exhibited a half-time of reactivation of 41 min (k_{obs} = 0.0168 ± 0.0003 $min^{-1}\,mM^{-1}$), approximately 66-fold faster than that observed without the oxime (see Fig. 6A). In addition, similar to spontaneous reactivation, the maximal recovery of hCE1 that was observed in the presence of DAM was 89 ± 4%. Thus, the neutral oxime DAM increased the rate of reactivation of sarin-inhibited hCE1 by more than 65-fold.

We next examined the ability of DAM to enhance the reactivation of hCE1 inhibited with pure enantiomeric P_R or P_S isoforms of the nerve agent analogs (see Fig. 1). We found that hCE1 inhibited with the P_S sarin analog exhibited reactivation with a half-time of 30 min (k_{obs} = 0.023 ± 0.004 $min^{-1}\,mM^{-1}$), whereas hCE1 inhibited by the P_R sarin analog exhibited no detectable reactivation (Fig. 6C). In contrast, hCE1 samples inhibited with P_S soman and cyclosarin analogs were capable of marginal reactivation, whereas respective P_R analogs displayed no recovery (Fig. 6, D and E). Taken together, these data suggest that the reactivation of hCE1 in the presence of the sarin analog was due to the hydrolysis of the P_S isomer, whereas the P_R isomer cannot be removed from the active site even in the presence of DAM.

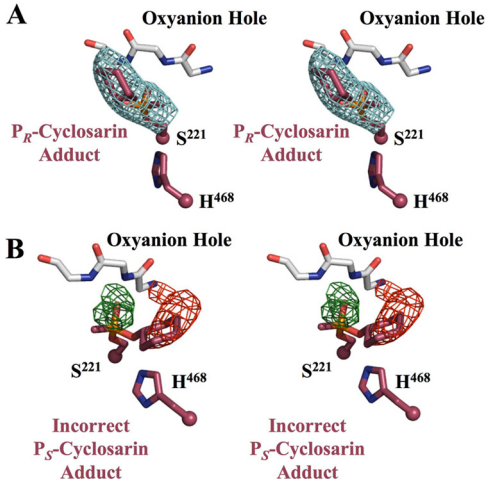

Fig. 4. hCE1-cyclosarin adduct stereochemistry. Ser221 and His468 of the catalytic triad and the cyclosarin adduct are shown in purple. The oxyanion hole is colored white. A, stereoview of a 3.1-Å resolution $F_o - F_c$ simulated annealing omit map (blue, contoured to 5 σ) calculated for the P_R-cyclosarin adduct. B, stereoview of initial difference density maps for the incorrect P_S-cyclosarin adduct (green for positive, shown at 3 σ; red for negative, shown at −3 σ).

Aging in OP-Inhibited hCE1. Aging in serine hydrolases involves the time-dependent dealkylation of the bound adduct, resulting in a permanently phosphorylated catalytic serine residue (Li et al., 2007). This process is rapid for soman in the active site of AChE ($t_{1/2}$ of ~2 min) and is the primary cause of the toxicity of this agent (Sanson et al., 2009). Once aging has occurred, nerve agent adducts are inert, even to strong oximes. We explored the propensity of hCE1 to age in the presence of nerve agent analog P_S stereoisomers by measuring the loss in the maximal level of DAM-mediated reactivation (A_{max}) over time. If the nerve agent analog adduct undergoes time-dependent dealkylation, one would expect an exponential decay for A_{max} (Shafferman et al., 1996). Over 48 h, no change in A_{max} was observed for any of the agent analogs (Fig. 6F). For example, after 2-h exposure of hCE1 to the P_S sarin analog, DAM was capable of reactivating ~60% of the enzyme activity (see Fig. 6B); however, even after 46 additional hours of incubation with this sarin analog, the same fraction of enzyme activity, recovered by DAM, was observed (see Fig. 6F). Thus, sarin-inhibited hCE1 does not seem to undergo the same first-order aging process that has been observed with other serine hydrolases, such as AChE.

Discussion

Organophosphorus nerve agents inactivate the neurotransmitter-regulating enzyme acetylcholinesterase and bind to other physiologically important proteins, such as albumin,

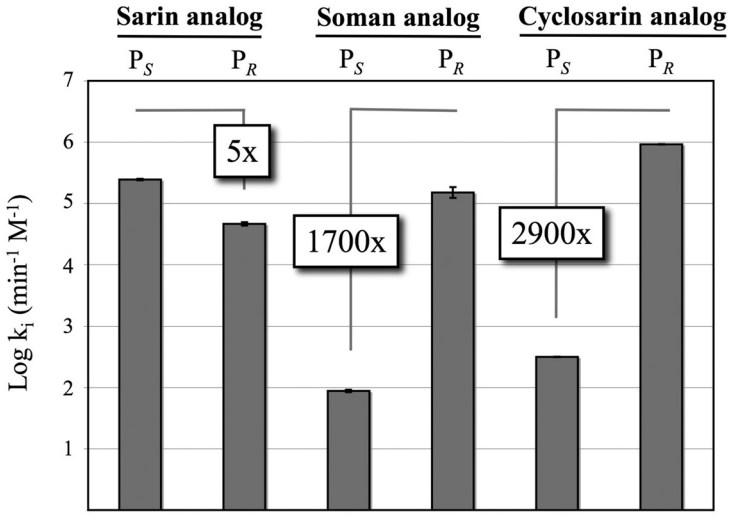

Analog Type		k_i ($s^{-1}\,M^{-1}$)	K_d (M)	k_2 (s^{-1})	P_R/P_S
Sarin	P_S	$4.10 \pm 0.10 \times 10^3$	$3.70 \pm 0.20 \times 10^{-7}$	$1.53 \pm 0.02 \times 10^{-3}$	0.190
	P_R	$0.77 \pm 0.05 \times 10^3$	$1.40 \pm 0.20 \times 10^{-6}$	$1.12 \pm 0.01 \times 10^{-3}$	
Soman	P_S	1.46 ± 0.07	$8.00 \pm 2.00 \times 10^{-4}$	$1.20 \pm 0.01 \times 10^{-3}$	1705
	P_R	$2.50 \pm 0.50 \times 10^3$	$2.20 \pm 0.20 \times 10^{-7}$	$0.55 \pm 0.05 \times 10^{-3}$	
Cyclosarin	P_S	5.27 ± 0.07	$1.70 \pm 0.20 \times 10^{-3}$	$9.00 \pm 0.83 \times 10^{-3}$	2900
	P_R	$1.53 \pm 0.12 \times 10^4$	$3.20 \pm 0.10 \times 10^{-7}$	$5.30 \pm 0.50 \times 10^{-3}$	

Fig. 5. Bimolecular rates of inhibition (k_i) for hCE1 and nerve agent analogs. Plotted as log k_i, hCE1 exhibits strong enantiomeric P_R preference for soman and cyclosarin analogs, with only slight P_S sarin analog selectivity. Dissociation constants (K_d) are similar to authentic nerve agents, whereas phosphorylation rates (k_2) are 2 to 3 orders of magnitude slower. (n = 3, S.E.)

lipases, and carboxylesterases (Fleming et al., 2007; Li et al., 2008). As such, these toxins are among the deadliest compounds developed by humans. The U.S. military has pursued the development of enzyme therapies capable of protecting personnel from nerve agent exposure (Lenz et al., 2007). In this report, we present X-ray crystallographic and biochemical data designed to evaluate the ability of hCE1 to act as potential enzyme-based therapeutic for nerve agent detoxification. Although we have previously determined crystal structures of hCE1 in complexes with soman and tabun (Fleming et al., 2007), here we report the novel crystal structure of hCE1 inhibited by cyclosarin (Fig. 2), one of the most potent inhibitors of human AChE (Gray and Dawson, 1987). Difference density and simulated annealing omit maps facilitated the placement of a covalent adduct with P_R stereochemistry bound to the catalytic Ser221 of hCE1 (Fig. 3A). After covalent adduction of OP nerve agents and analogs to the catalytic serine, stereochemistry at the phosphorus atom remains the same. A rearrangement in priority assignment after collapse of the pentahedral intermediate causes the covalent phosphonyl-enzyme intermediate to retain the original stereochemistry of the OP compound before enzyme binding (Epstein et al., 2009). Therefore, the P_R stereochemistry observed in the crystal structure of the hCE1-cyclosarin acyl-enzyme adduct (see Figs. 3 and 4) corresponds to the preferential reaction of hCE1 with the P_R analog of cyclosarin.

Indeed, using thiomethyl-substituted nerve agent analogs, we were able to complete experiments designed to examine the stereoselectivity of hCE1 for these analogs of sarin, soman, and cyclosarin (Fig. 4). We found that hCE1 preferentially binds to the P_R isomers of cyclosarin and soman analogs, which is opposite to the stereopreference observed for AChE with bona fide nerve agents. A structural comparison of the hCE1-soman and hCE1-cyclosarin crystal structures with AChE-soman (RCSB PDB access code 2wgo; Sanson et al., 2009) reveals that the bulky P_R *O*-alkoxy group is positioned into the larger hydrophobic binding pocket of hCE1. In contrast, this region is occupied in AChE by a long acyl loop that dips into the active site pocket and precludes binding of P_R nerve agents (Fleming et al., 2007; Sanson et al., 2009). Therefore, the geometry of the hCE1 active site size dictates the enantiomeric binding of the bulkier nerve agents soman and cyclosarin. With the smaller nerve agent sarin, hCE1 demonstrated only a 5-fold preference for the P_S isomer of the sarin nerve agent analog (Fig. 5). Our structures indicate that although both isomers of sarin will fit in the active site of the enzyme, only P_S sarin is capable of forming stabilizing hydrophobic contacts with Phe101 and Leu97; P_R sarin

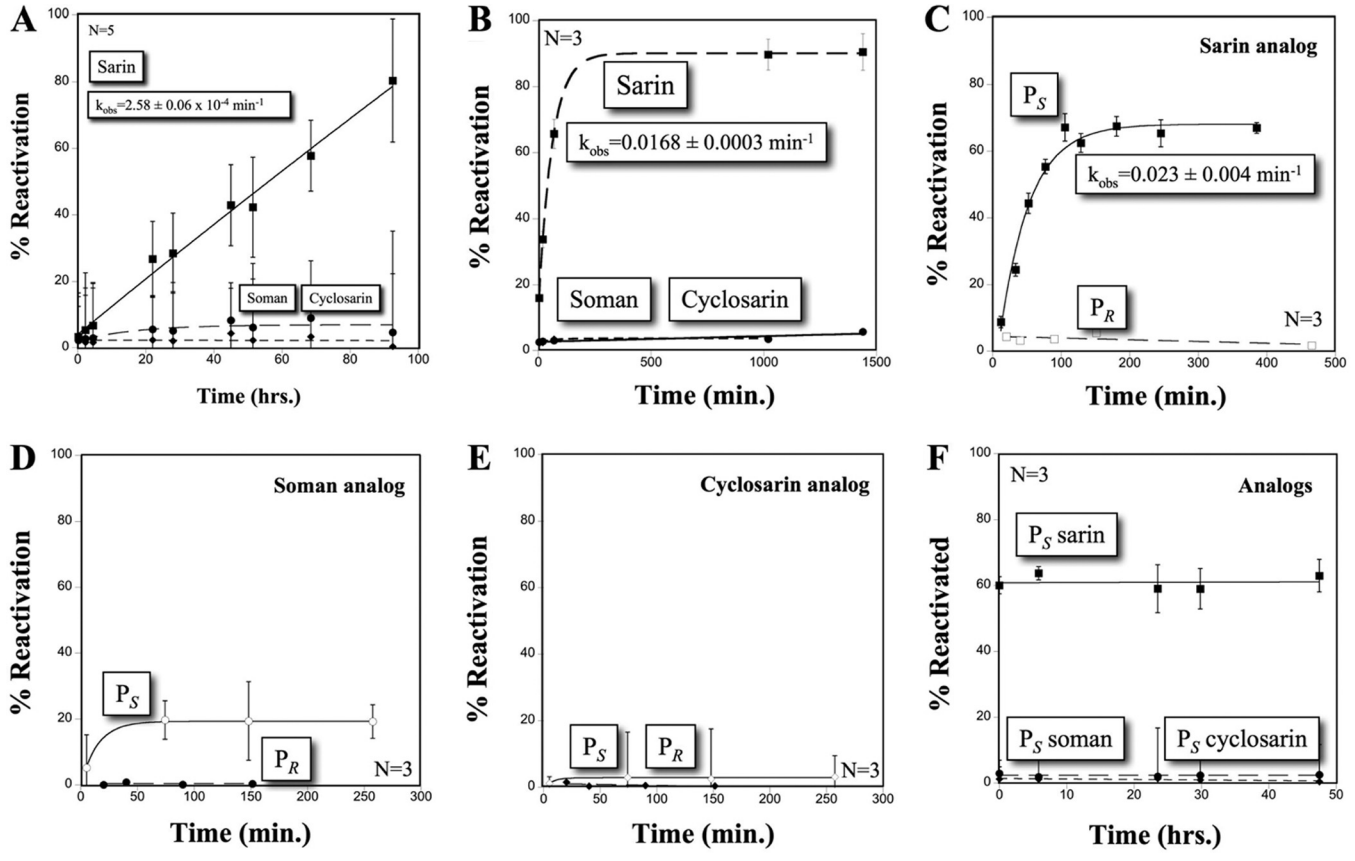

Fig. 6. hCE1 reactivation after inhibition by racemic bona fide OP nerve agents or stereospecific nerve agent analogs. A, spontaneous reactivation of racemic bona fide OP agents. Reactivation only occurs with sarin (■), with a half-time of reactivation of 45 h (n = 5, S.D.). Soman (●) and cyclosarin (♦) remained permanently inhibited. B, DAM-assisted reactivation with racemic bona fide nerve agents. Reactivation is only measured against sarin (■) with a half-time of reactivation of 41 min (n = 3, S.E.). Soman (●) and cyclosarin (♦) did not reactivate. C, DAM-assisted reactivation of sarin analogs. The P_S isomer (■) reactivates with a half-time of 30 min (n = 3, S.E.). P_R sarin (□) analog did not reactivate. D, DAM-assisted reactivation of soman analogs. The greatest reactivation was measured in the P_S (○) enantiomer, whereas the P_R (●) analog remained inhibited. E, DAM, assisted reactivation of cyclosarin analogs. Negligible reactivation was measured for either P_S (◇) or P_R (♦) cyclosarin analog. F, determination of aging with P_S nerve agent analogs; no aging was measured for the P_S species.

would not form analogous interactions (Fig. 7A). These structural considerations, in part, explain the observed strong preference for P_R soman and cyclosarin and the relatively weak preference for P_S sarin exhibited by hCE1.

After the formation of the acyl-enzyme intermediate, the first step of the serine hydrolase catalytic mechanism (see Fig. 3A), nerve agent-esterase complexes can undergo reactivation or aging. Both spontaneous and oxime-assisted reactivation displaces the acyl-enzyme intermediate and restores the enzyme to normal function. We found that nerve agent-inhibited hCE1 only reactivates spontaneously, or with the oxime DAM, after incubation with sarin (Fig. 6, A and B). In addition, although DAM enhanced the rate of reactivation 66-fold, both spontaneous and oxime-assisted reactivation only restores ~85% of the original enzyme activity. Using the stereogenic nerve agent analogs, we showed that the rate of DAM-assisted reactivation after inhibition with the P_S sarin analog was identical, within error, with the rate of DAM-assisted reactivation for racemic sarin (Fig. 6, B and C). No recovery was measured for the P_R sarin analog (Fig. 6C). In contrast to sarin, hCE1 incubated with racemic samples of the nerve agents soman or cyclosarin exhibited relatively little reactivation (Fig. 6, A and B). Furthermore, only weak reactivation was only achieved with the P_S isomers when analogs of these nerve agents were incubated with hCE1 (Fig. 6, D and E). Based on these data, we conclude that hCE1 stereoselectively reactivates P_S sarin after racemic inhibition.

We next modeled how hCE1 might preferentially reactivate in the presence of P_S sarin (Fig. 7B). Previous work investigating the influence of pH on spontaneous reactivation in AChE identified the importance of two ionizable residues with pK_a values of 6.9 and 9.8, suggesting possible histidine and tyrosine residues, respectively (Reiner and Aldridge, 1967). In the hCE1 active site, the catalytic His468 neighbors P_S sarin and Tyr152 are located approximately 8 Å away. These two residues are connected via a hydrogen-bonding network through Glu200 (Fig. 7B). It has been observed in the structure of the AChE covalent complex with nonaged P_S *O*-ethyl *S*-(2-diisopropylaminoethyl) methylphosphonothioate that the protonated Nε2 of His440 (His468 in hCE1) rotates away from Ser200 (Ser221 in hCE1) to form a hydrogen-bond with Glu199 (Glu220 in hCE1) (Millard et al., 1999). The Nε2 movement would be expected to be blocked in hCE1 by larger alkoxy groups, such as the *O*-pinacolyl group in soman, and is not observed in the nonaged AChE soman structure (Sanson et al., 2009). If this shift occurs in hCE1 with P_S sarin, however, the His468 Nε2 rotation to Glu220 would reorient the remaining His468 nitrogen, Nδ1, formerly hydrogen-bonded to Glu354. It would then be positioned to interact with the P_S sarin O2 atom and may act as a general base for hydrolytic dephosphonylation (Fig. 7B). An analogous orientation of the O2 atom of P_R sarin would not be possible while still maintaining interactions with the oxyanion hole (see Fig. 7A). By this model, hCE1 will only reactivate after inhibition with P_S sarin, consistent with the experimental results presented above. However, the rate of reactivation is observed to be poor, probably because of the weak nucleophilicity of Tyr152 at pH 7.4.

Organophosphinate-esterase complexes may also undergo aging. Although P_S isomers of OPs showed some capability to be removed from the hCE1 active site by reactivation (Fig. 6, C–E), we saw no evidence for first-order aging in hCE1 (Fig. 6F). We therefore considered what the fate of the P_R-hCE1 adducts is if they do not age and the state of the remaining percentage of P_S-hCE1 adducts that do not undergo reactivation. For complexes of P_R organophosphates and hCE1, we propose that they remain at the acyl-enzyme intermediate stage of the enzyme's reaction mechanism. This state has been observed in the hCE1-P_R soman and hCE1-P_R cyclosarin crystal structures and via matrix-assisted laser desorption ionization/time of flight analysis of BuChE inhibited by P_R analogs of sarin, soman, and cyclosarin (Gilley et al., 2009). For the 40% of P_S-sarin analog complexes with hCE1 that do not undergo reactivation, we propose that an alternate Ser221 state is created. In addition to forming adducts identical with authentic agents, the thiomethyl-nerve agent analogs used in this study have been shown to undergo a unique reaction, in which the *O*-alkoxy rather than the thiomethyl group is displaced upon collapse of the original pentahedral intermediate (Gilley et al., 2009). Therefore, dehydroalanine formation at the catalytic serine might also occur with these nerve agent analogs. Mass spectrometry studies were attempted to confirm or deny the presence of this adduct in hCE1; unfortunately, the peptide fragment containing Ser221 could not be isolated, and no useful data were obtained (O. Lockridge, personal communication).

In summary, these studies establish the stereopreference of wild-type hCE1 for nerve agent analogs of cyclosarin, soman, and sarin and confirm this preference for cyclosarin with crystallographic data. In addition, they indicate that the native form of hCE1 is capable of reactivation after incubation with the nerve agent sarin and that the rate of reactivation is enhanced with the neutral oxime DAM. In future studies, we will use these data to design mutant forms of

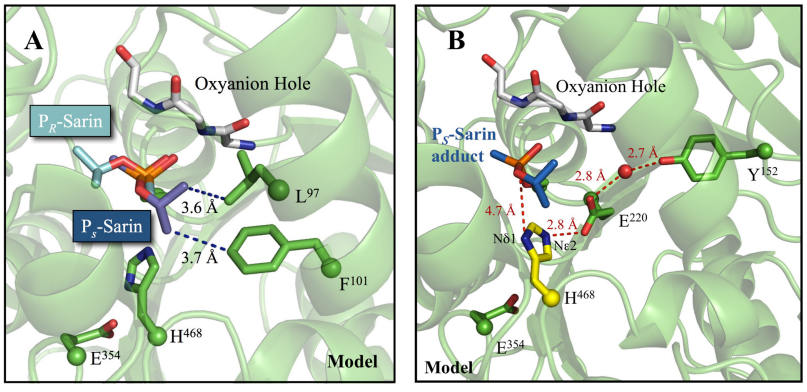

Fig. 7. hCE1-sarin model. A, P_R and P_S enantiomers of sarin modeled in the hCE1 active site. The *O*-isopropyl group on P_S sarin makes hydrophobic contacts with Phe101 and Leu97, whereas P_R does not have any additional interactions. B, model of proposed mechanism of P_S sarin reactivation in hCE1. In AChE, His468 has been observed to rotate away from Glu354 and interact with Glu221 after acylation. Modeling this shift in the hCE1 active site, there is an electronic network formed between Tyr152 (green) and His468 (yellow) that may either deprotonate Nε2 or allow Nδ1 of His468 to act as a general base for water activation. P_S sarin (blue) was modeled into the hCE1-soman structure (RCSB PDB access code 2hrq; Fleming et al., 2007).

hCE1 with the goal of enhancing nerve agent hydrolysis not only for sarin but also for soman and cyclosarin.

Acknowledgments

We thank the Redinbo Lab, particularly Dr. Sarah Kennedy and Rebekah Nash, for assistance in X-ray data collection and manuscript preparation.

References

Aurbek N, Thiermann H, Szinicz L, Eyer P, and Worek F (2006) Analysis of inhibition, reactivation and aging kinetics of highly toxic organophosphorus compounds with human and pig acetylcholinesterase. *Toxicology* **224:**91–99.

Bartling A, Worek F, Szinicz L, and Thiermann H (2007) Enzyme-kinetic investigation of different sarin analogues reacting with human acetylcholinesterase and butyrylcholinesterase. *Toxicology* **233:**166–172.

Bencharit S, Morton CL, Howard-Williams EL, Danks MK, Potter PM, and Redinbo MR (2002) Structural insights into CPT-11 activation by mammalian carboxylesterases. *Nat Struct Biol* **9:**337–342.

Bencharit S, Morton CL, Hyatt JL, Kuhn P, Danks MK, Potter PM, and Redinbo MR (2003) Crystal structure of human carboxylesterase 1 complexed with the Alzheimer's drug tacrine: from binding promiscuity to selective inhibition. *Chem Biol* **10:**341–349.

Brünger AT, Adams PD, Clore GM, DeLano WL, Gros P, Grosse-Kunstleve RW, Jiang JS, Kuszewski J, Nilges M, Pannu NS, et al. (1998) Crystallography & NMR system: A new software suite for macromolecular structure determination. *Acta Crystallogr D Biol Crystallogr* **54:**905–921.

Collaborative Computational Project and Number 4 (1994) The CCP4 suite: programs for protein crystallography. *Acta Crystallogr D Biol Crystallogr* **50:**760–763.

Doctor BP and Saxena A (2005) Bioscavengers for the protection of humans against organophosphate toxicity. *Chem Biol Interact* **157:**167–171.

Dunn MA and Sidell FR (1989) Progress in medical defense against nerve agents. *JAMA* **262:**649–652.

Emsley P and Cowtan K (2004) Coot: model-building tools for molecular graphics. *Acta Crystallogr D Biol Crystallogr* **60:**2126–2132.

Epstein TM, Samanta U, Kirby SD, Cerasoli DM, and Bahnson BJ (2009) Crystal structures of brain group-VIII phospholipase A2 in nonaged complexes with the organophosphorus nerve agents soman and sarin. *Biochemistry* **48:**3425–3435.

Fleming CD, Edwards CC, Kirby SD, Maxwell DM, Potter PM, Cerasoli DM, and Redinbo MR (2007) Crystal structures of human carboxylesterase 1 in covalent complexes with the chemical warfare agents soman and tabun. *Biochemistry* **46:**5063–5071.

Forsberg A and Puu G (1984) Kinetics for the inhibition of acetylcholinesterase from the electric eel by some organophosphates and carbamates. *Eur J Biochem* **140:**153–156.

Gilley C, MacDonald M, Nachon F, Schopfer LM, Zhang J, Cashman JR, and Lockridge O (2009) Nerve agent analogues that produce authentic soman, sarin, tabun, and cyclohexyl methylphosphonate-modified human butyrylcholinesterase. *Chem Res Toxicol* **22:**1680–1688.

Gray AP (1984) Design and structure-activity relationships of antidotes to organophosphorus anticholinesterase agents. *Drug Metab Rev* **15:**557–589.

Gray PJ and Dawson RM (1987) Kinetic constants for the inhibition of eel and rabbit brain acetylcholinesterase by some organophosphates and carbamates of military significance. *Toxicol Appl Pharmacol* **91:**140–144.

Heidari R, Devonshire AL, Campbell BE, Bell KL, Dorrian SJ, Oakeshott JG, and Russell RJ (2004) Hydrolysis of organophosphorus insecticides by in vitro modified carboxylesterase E3 from *Lucilia cuprina*. *Insect Biochem Mol Biol* **34:**353–363.

Jokanović M (2009) Current understanding of the mechanisms involved in metabolic detoxification of warfare nerve agents. *Toxicol Lett* **188:**1–10.

Kabsch W (1988) Evaluation of single-crystal X-ray diffraction data from a position-sensitive detector. *J Appl Crystallogr* **21:**916–924.

Kovarik Z, Radić Z, Berman HA, Simeon-Rudolf V, Reiner E, and Taylor P (2003) Acetylcholinesterase active centre and gorge conformations analysed by combinatorial mutations and enantiomeric phosphonates. *Biochem J* **373:**33–40.

Langenberg JP, De Jong LP, Otto MF, and Benschop HP (1988) Spontaneous and oxime-induced reactivation of acetylcholinesterase inhibited by phosphoramidates. *Arch Toxicol* **62:**305–310.

Laskowski R, MacArthur M, Moss D, and Thornton J (1993) PROCHECK: a program to check the stereochemical quality of protein structures. *J Appl Crystallogr* **26:**283–291.

Lenz DE, Yeung D, Smith JR, Sweeney RE, Lumley LA, and Cerasoli DM (2007) Stoichiometric and catalytic scavengers as protection against nerve agent toxicity: a mini review. *Toxicology* **233:**31–39.

Li B, Nachon F, Froment MT, Verdier L, Debouzy JC, Brasme B, Gillon E, Schopfer LM, Lockridge O, and Masson P (2008) Binding and hydrolysis of soman by human serum albumin. *Chem Res Toxicol* **21:**421–431.

Li H, Schopfer LM, Nachon F, Froment MT, Masson P, and Lockridge O (2007) Aging pathways for organophosphate-inhibited human butyrylcholinesterase, including novel pathways for isomalathion, resolved by mass spectrometry. *Toxicol Sci* **100:**136–145.

Maxwell DM (1992) The specificity of carboxylesterase protection against the toxicity of organophosphorus compounds. *Toxicol Appl Pharmacol* **114:**306–312.

Maxwell DM and Brecht KM (2001) Carboxylesterase: specificity and spontaneous reactivation of an endogenous scavenger for organophosphorus compounds. *J Appl Toxicol* **21 (Suppl 1):**S103–S107.

Maxwell DM, Brecht KM, Doctor BP, and Wolfe AD (1993) Comparison of antidote protection against soman by pyridostigmine, HI-6 and acetylcholinesterase. *J Pharmacol Exp Ther* **264:**1085–1089.

Maxwell DM, Lieske CN, and Brecht KM (1994) Oxime-induced reactivation of carboxylesterase inhibited by organophosphorus compounds. *Chem Res Toxicol* **7:**428–433.

Millard CB, Kryger G, Ordentlich A, Greenblatt HM, Harel M, Raves ML, Segall Y, Barak D, Shafferman A, Silman I, et al. (1999) Crystal structures of aged phosphonylated acetylcholinesterase: nerve agent reaction products at the atomic level. *Biochemistry* **38:**7032–7039.

Morton CL and Potter PM (2000) Comparison of *Escherichia coli*, *Saccharomyces cerevisiae*, *Pichia pastoris*, *Spodoptera frugiperda*, and COS7 cells for recombinant gene expression. Application to a rabbit liver carboxylesterase. *Mol Biotechnol* **16:**193–202.

Newmark J (2007) Nerve agents. *Neurologist* **13:**20–32.

Okumura T, Hisaoka T, Yamada A, Naito T, Isonuma H, Okumura S, Miura K, Sakurada M, Maekawa H, Ishimatsu S, et al. (2005) The Tokyo subway sarin attack–lessons learned. *Toxicol Appl Pharmacol* 207 (2 Suppl):471–476.

Redinbo MR and Potter PM (2005) Mammalian carboxylesterases: from drug targets to protein therapeutics. *Drug Discov Today* **10:**313–325.

Reeves TE, Wales ME, Grimsley JK, Li P, Cerasoli DM, and Wild JR (2008) Balancing the stability and the catalytic specificities of OP hydrolases with enhanced V-agent activities. *Protein Eng Des Sel* **21:**405–412.

Reiner E and Aldridge WN (1967) Effect of pH on inhibition and spontaneous reactivation of acetylcholinesterase treated with esters of phosphorus acids and of carbamic acids. *Biochem J* **105:**171–179.

Sanson B, Nachon F, Colletier JP, Froment MT, Toker L, Greenblatt HM, Sussman JL, Ashani Y, Masson P, Silman I, et al. (2009) Crystallographic snapshots of nonaged and aged conjugates of soman with acetylcholinesterase, and of a ternary complex of the aged conjugate with pralidoxime. *J Med Chem* **52:**7593–7603.

Shafferman A, Ordentlich A, Barak D, Stein D, Ariel N, and Velan B (1996) Aging of phosphylated human acetylcholinesterase: catalytic processes mediated by aromatic and polar residues of the active centre. *Biochem J* **318:**833–840.

Trapp R (2006) Worldwide governmental efforts to locate and destroy chemical weapons and weapons materials: minimizing risk in transport and destruction. *Ann NY Acad Sci* **1076:**527–539.

Volans AP (1996) Sarin: guidelines on the management of victims of a nerve gas attack. *J Accid Emerg Med* **13:**202–206.

Wierdl M, Tsurkan L, Hyatt JL, Edwards CC, Hatfield MJ, Morton CL, Houghton PJ, Danks MK, Redinbo MR, and Potter PM (2008) An improved human carboxylesterase for enzyme/prodrug therapy with CPT-11. *Cancer Gene Ther* **15:**183–192.

Address correspondence to: Dr. Matthew R. Redinbo, Department of Chemistry, CB #3290, University of North Carolina at Chapel Hill, Chapel Hill, NC 27599-3290. E-mail: redinbo@unc.edu